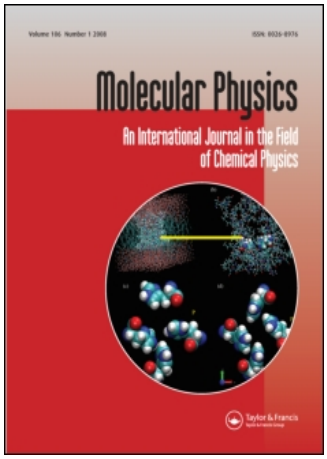

Molecular Physics
An International Journal in the Field of Chemical Physics
Publication details, including instructions for authors and subscription information:
http://www.informaworld.com/smpp/title~content=t713395160

Ultrasoft colloids in cavities of oscillating size or sharpness

M. Rex [a]; C. N. Likos [a]; H. LÖwen [a]; J. Dzubiella [b]
[a] Institut für Theoretische Physik II, Heinrich-Heine-Universität Düsseldorf, D-40225 Düsseldorf, Germany
[b] NSF Center for Theoretical Biological Physics (CTBP), Department of Chemistry and Biochemistry, University of California, San Diego, La Jolla, California 92093-0365, USA

Online Publication Date: 20 February 2006
To cite this Article: Rex, M., Likos, C. N., LÖwen, H. and Dzubiella, J. (2006) 'Ultrasoft colloids in cavities of oscillating size or sharpness', Molecular Physics, 104:4, 527 - 540
To link to this article: DOI: 10.1080/00268970500460382
URL: http://dx.doi.org/10.1080/00268970500460382

Molecular Physics, Vol. 104, No. 4, 20 February 2006, 527–540

Ultrasoft colloids in cavities of oscillating size or sharpness

M. REX†, C. N. LIKOS*†, H. LÖWEN† and J. DZUBIELLA‡

†Institut für Theoretische Physik II, Heinrich-Heine-Universität Düsseldorf, Universitätsstraße 1, D-40225 Düsseldorf, Germany

‡NSF Center for Theoretical Biological Physics (CTBP), Department of Chemistry and Biochemistry, University of California, San Diego, La Jolla, California 92093-0365, USA

(*Received 25 October 2005; in final form 7 November 2005*)

We employ dynamical density functional theory (DDFT) and Brownian Dynamics (BD) simulations to examine the fully developed dynamics of ultrasoft colloids interacting via a Gaussian pair potential in time-dependent external fields. The DDFT formalism employed is that of Marconi and Tarazona [*J. Chem. Phys.*, **110**, 8032 (1999)], which allows for determination of the time-dependent density profile based on knowledge of the static, equilibrium density functional. Three different dynamical situations are examined: firstly, the behaviour of Gaussian particles in a spherical cavity of oscillating size, including both sudden and continuous changes in the size of the cavity. Secondly, a spherical cavity with a fixed size but varying sharpness. Finally, to investigate a strong inhomogeneity in the density profile we study the diffusion of one layer of particles which is initially strongly confined and separated from the remaining system via an external potential. In all cases, DDFT is in excellent agreement with BD results, demonstrating the applicability of the theory to dynamical problems involving overdamped interacting particles in a solvent.

1. Introduction

Equilibrium density functional theory (DFT), as formulated in the domain of classical statistical mechanics [1], has proved to be a highly successful tool in analysing a variety of phenomena associated with the behaviour of classical inhomogeneous fluids. The quantity of central interest in DFT is the ensemble-averaged one-particle density $\rho(\mathbf{r})$, which depends on the spatial coordinate $\mathbf{r}$, reflecting the system's inhomogeneity, and it is, evidently, time-independent. Spatially inhomogeneous density profiles arise in a variety of physical situations: they can be induced by spatially dependent external fields $V_{\text{ext}}(\mathbf{r})$ (fluids in contact with walls or under the influence of other external fields), imposed by suitably chosen thermodynamic and boundary conditions (fluid–fluid interfaces between coexisting phases), or even emerge as states of spontaneously broken symmetry in phase transitions (crystallization). The formalism of classical DFT rests on the uniqueness of the intrinsic Helmholtz free energy functional $\Phi[\rho]$ for a given interaction potential between the particles. Further, the equilibrium density profile minimizes the value of the grand potential functional $\Omega[\rho] = \Phi[\rho] + \int \mathrm{d}\mathbf{r}[V_{\text{ext}}(\mathbf{r}) - \mu]\rho(\mathbf{r})$, where μ is the chemical potential. For consistency with what is to follow, we also define $F[\rho] \equiv \Phi[\rho] + \int \mathrm{d}\mathbf{r} V_{\text{ext}}(\mathbf{r})\rho(\mathbf{r})$, the sum of the intrinsic and external potential-contributions to an extended Helmholtz free energy functional $F[\rho]$.

Much less is known about classical fluids far from equilibrium. In this case the one-particle density acquires an explicit time dependence and becomes a spatiotemporal field $\rho(\mathbf{r}, t)$. This explicit time dependence can arise, e.g. in situations in which the system is driven from one equilibrium state to another (due to the lifting or imposition of a constraint) or is constantly held in a non-equilibrium state by the influence of a space- and time-dependent external field $V_{\text{ext}}(\mathbf{r}, t)$. The possibility of using equilibrium DFT, supplemented by a time-evolution operation, to describe the *dynamics* of a classical fluid is very appealing. Along these lines, Munakata has constructed a dynamical DFT [2], starting from phenomenological, hydrodynamic equations for the density $\rho(\mathbf{r}, t)$ and the momentum density $\mathbf{g}(\mathbf{r}, t)$ of a damped, Brownian fluid. The result of this approach is a first-order in time differential equation for $\rho(\mathbf{r}, t)$ that involves the *deterministic* free

*Corresponding author. Email: likos@thphy.uni-duesseldorf.de

Molecular Physics
ISSN 0026–8976 print/ISSN 1362–3028 online © 2006 Taylor & Francis
http://www.tandf.co.uk/journals
DOI: 10.1080/00268970500460382

energy functional $F[\rho]$ as well as a *random* contribution from the solvent-induced noise [2, 3]. Shortly thereafter, Dean [4] put forward another equation for the time evolution of the density field, which is similar to that of Munakata [2] in its form but it involves a *different* free energy functional, $H[\rho]$, which is *not* the one obtained in equilibrium DFT. Another dynamical equation for $\rho(\mathbf{r}, t)$ has been obtained in the approach of Marconi and Tarazona (MT) [5]. Here, the time–evolution equation is *completely deterministic* and it involves the equilibrium density functional $F[\rho]$. This is the theory used in this paper and will be elaborated upon in what follows.

The apparent contradictions between the various dynamical equations were clarified in the recent works by Archer and Rauscher [6] and by Yoshimori [7]. Archer and Rauscher focused their attention exclusively on Brownian particles, taking as a starting point the N coupled Langevin equations for the N interacting particles. They then showed that the presence or absence of random contributions in the dynamical equation depends on the definition of the one-particle density field. If one focuses on the *ensemble-averaged*, time-dependent one-particle density $\rho(\mathbf{r}, t)$ *without* involving coarse-graining, then the dynamical equation of motion should be deterministic. Under additional, physical assumptions the dynamical density functional theory (DDFT) of MT follows [6]. The equation of Dean [4] holds for the non-ensemble-averaged density operator $\hat{\rho}(\mathbf{r}, t)$, and it includes noise terms, as also does the equation of Munakata [2], which describes the evolution of a coarse-grained density field $\bar{\rho}(\mathbf{r}, t)$. Yoshimori, on the other hand, started from the Liouville equation using a microscopic Hamiltonian [7], and applied a projection-operator formalism, reaching similar conclusions to Archer and Rauscher [6]. Another important recent development has been the proof by Chan and Finken [8] that a stationary action principle for the time-dependent density exists. Chan and Finken were also able to recover the DDFT equations of [4, 5] by employing a suitably-defined adiabatic limit.

The DDFT of Marconi and Tarazona has attracted considerable attention recently for various reasons. On the one hand, its deterministic character renders the solution of the differential equation simpler than in other approaches. On the other hand, the existence of accurate Helmholtz free energy functionals for a number of model systems allows for testing the DDFT for a variety of time-dependent external potentials. In the original paper of Marconi and Tarazona [5], they applied their DDFT to a driven, one-dimensional, hard-rod system, for which the equilibrium free energy functional is exactly known. Dzubiella and Likos [9] examined the relaxation dynamics of soft colloids under sudden expansion- and compression-processes. Penna and co-workers analysed the steady-state dynamics of colloidal particles in narrow channels [10] as well as the density profile of a polymer bath through which a colloidal particle is pulled with constant speed [11]. The problem of *two* colloids driven in a bath of polymer coils and the associated dynamical depletion force has been examined by Dzubiella *et al*. [12]. Archer and Evans applied the DDFT formalism to the problem of spinodal decomposition of a phase-separating fluid [13], and, most recently, Archer extended the DDFT to mixtures, studying the dynamics of a binary phase-separating fluid of Gaussian particles in a cavity [14]. Finally, Rex *et al*. have studied ultrasoft colloids driven by travelling fields and sheared between two topographically patterned walls [15].

In all the aforementioned studies, excellent agreement between the DDFT and simulation results was found. It is important to emphasize that accurate static functionals were employed throughout, so that the conclusion can be drawn that the dynamics of Brownian fluids is governed by their statics. Yet, the dynamical situations examined were either relaxative (sudden quenching or expansion [9, 13, 14]) or of steady-state nature, in which the density field depends on space and time solely through the combination $\mathbf{r} - \mathbf{c}t$, $\mathbf{c}$ denoting the velocity of a colloidal particle driven through the system or of some external, travelling wave [10–12, 15]. The dynamics of fluids under the influence of external fields arbitrarily varying both in space and in time has not yet been investigated with the DDFT formalism. It is the purpose of this paper to address precisely this question, by considering ultrasoft, Gaussian colloids in cavities of *constantly* varying shape or sharpness. This paper is organized as follows: in section 2 we present a concise derivation of the DDFT formalism and we discuss the conditions under which hydrodynamic interactions can be ignored. In section 3 we present and discuss our results for various time-dependent external fields, whereas in section 4 we examine the question of the diffusion of a single layer of ultrasoft particles in the bulk of the rest of the fluid. Finally, in section 5 we summarize and draw our conclusions.

2. Dynamical density functional theory (DDFT)

2.1. *The formalism*

The DDFT equation of Marconi and Tarazona [5] can be derived in various different ways. The first route, which has been followed in the original derivation of [5], starts from the Langevin equations of motion. Archer and Evans [13], as well as Archer [14] have put forward an alternative derivation, which has as a point of

departure the Smoluchowski equation. The latter describes the time evolution of the probability density function of N Brownian particles. In the derivation of [13] and [14] it has been shown that the DDFT equation holds in full generality, i.e. when many-body interactions between the constituent particles are present. The crucial approximation which has to be made in both approaches is that the equal-time two point correlations in the time-dependent systems are identical to an equilibrium system that has a static, one-particle density $\rho_{\mathrm{eq}}(\mathbf{r})$ equal to the instantaneous density field $\rho(\mathbf{r}, t)$ of the dynamical system. Yoshimori [7] termed this a *local equilibrium condition* and has shown that it naturally arises in a projection-operator formalism under the imposition of a Markovian approximation. Chan and Finken [8] argued that the DDFT equation results by the replacement of the exact, dynamical free energy functional with the equilibrium one and used, appropriately, the term *adiabatic approximation*. The latter seems physically reasonable for overdamped Brownian particles.

Each of the aforementioned derivations has its own merits, with some being mathematically more demanding than others. Here, we choose to present a brief description of the original steps leading to the DDFT equation [5], mainly on the grounds of simplicity and physical transparency. We consider an assembly of N Brownian particles, such as colloids in a microscopic solvent, whose coordinates are $\{\mathbf{r}_1, \mathbf{r}_2, \ldots, \mathbf{r}_N\}$. These particles are assumed to interact by means of an *effective* pair potential $V(|\mathbf{r}_i - \mathbf{r}_j|)$†. In addition, the colloids are under the influence of a time-dependent external potential $V_{\mathrm{ext}}(\mathbf{r}, t)$. We ignore hydrodynamic interactions (HI) for the moment, returning to a justification of this assumption later. In this case, the particles' coupled equations of motion are the following Langevin equations that read as:

$$\frac{\mathrm{d}\mathbf{r}_i(t)}{\mathrm{d}t} = -\Gamma\nabla_{\mathbf{r}_i}\left(\sum_{j\neq i} V(|\mathbf{r}_i - \mathbf{r}_j|) + V_{\mathrm{ext}}(\mathbf{r}_i, t)\right) + \mathbf{w}_i(t). \quad (1)$$

Here, Γ is a mobility coefficient originating from the solvent and $\mathbf{w}_i(t) = \left(w_i^x, w_i^y, w_i^z\right)$ is a stochastic Gaussian noise term representing the random collisions with the solvent molecules and having the properties

$$\langle \mathbf{w}_i(t)\rangle = 0\,, \quad (2)$$

$$\langle w_i^\alpha(t) w_i^\beta(t')\rangle = 2D\delta_{\alpha\beta}\delta(t - t')\,, \quad (3)$$

where $\langle \ldots \rangle$ denotes the average over the Gaussian noise distribution and $\alpha, \beta = x, y, z$ are the Cartesian components. D is the Stokes–Einstein diffusion coefficient, for which the Einstein relation gives $\Gamma/D = (k_{\mathrm{B}}T)^{-1} \equiv \beta$, where $k_{\mathrm{B}}T$ is the thermal energy. Applying the rules of the Itô stochastic calculus [4] to equation (1) and taking the average over all realizations of the stochastic noise, the Langevin equations give

$$\Gamma^{-1}\frac{\partial\rho(\mathbf{r}, t)}{\partial t} = \nabla_{\mathbf{r}}\cdot\left[\beta^{-1}\nabla_{\mathbf{r}}\rho(\mathbf{r}, t) + \rho(\mathbf{r}, t)\nabla_{\mathbf{r}}V_{\mathrm{ext}}(\mathbf{r}, t)\right] + \nabla_{\mathbf{r}}\cdot\int \mathrm{d}\mathbf{r}'\,\langle\hat{\rho}(\mathbf{r}, \mathrm{t})\hat{\rho}(\mathbf{r}', \mathrm{t})\rangle\nabla_{\mathbf{r}}\mathrm{V}(|\mathbf{r} - \mathbf{r}'|). \quad (4)$$

Here, $\hat{\rho}(\mathbf{r}, t) \equiv \sum_i \delta(\mathbf{r}_i(t) - \mathbf{r})$ is the usual one-particle density operator and $\rho(\mathbf{r}, t) = \langle\hat{\rho}(\mathbf{r}, t)\rangle$ is its expectation value, averaged over all realizations of the noise. The right-hand side involves the equal-time two-particle distribution function $\rho^{(2)}(\mathbf{r}, \mathbf{r}', t) \equiv \langle\hat{\rho}(\mathbf{r}, t)\hat{\rho}(\mathbf{r}', t)\rangle$, which is itself a noise-averaged quantity. Thus, equation (4) is a relation between noise-averaged quantities, in which random noise contributions are absent, and is therefore deterministic in nature. Equation (4) is exact but its form is not closed: it relates the time evolution of the one-body quantity $\rho(\mathbf{r}, t)$ to the two-body correlation function $\rho^{(2)}(\mathbf{r}, \mathbf{r}', t)$. Following the same procedure, an equation for the time evolution of $\rho^{(2)}(\mathbf{r}, \mathbf{r}', t)$ can be obtained, which in turn involves the three-particle distribution function $\rho^{(3)}(\mathbf{r}, \mathbf{r}', \mathbf{r}'', t)$. In this way, one obtains an infinite hierarchy of relations, analogous to the Born–Bogoliubov–Green–Kirkwood–Yvon (BBGKY) equations [5].

In order to obtain closure to equation (4), Marconi and Tarazona [5] proposed a physical assumption, incorporating the density functional formalism into the theory: as the system follows its dynamical evolution, the equal-time two-particle correlations are approximated by those of a system in thermodynamic equilibrium with a *static* one-particle density $\rho_{\mathrm{eq}}(\mathbf{r})$ that is the same as the noise-averaged, instantaneous dynamical one-particle density $\rho(\mathbf{r}, t)$. This assumption is reasonable for Brownian fluids, for which the momentum degrees of freedom relax instantaneously and the local equilibrium condition [7] appears intuitively correct. The benefit arising from this assumption is that, in equilibrium, *all* correlation functions are *uniquely* determined by the one-particle density, due to the uniqueness of the free-energy functional $F[\rho]$;

†An effective potential includes both the direct interaction between mesoscopic, colloidal particles and the indirect interactions mediated by the microscopic, solvent degrees of freedom, which are assumed to have been integrated out. For a discussion of the notion of the effective potential, see, e.g. [16]. For the applicability of effective interactions in dynamical problems, see the discussion in [14].

in other words, the correlation functions are unique functionals of $\rho_{\mathrm{eq}}(\mathbf{r})$ [1, 5]. By extending the uniqueness property to dynamics, equation (4) can be cast into a form that involves exclusively the equilibrium Helmholtz free energy functional $F[\rho]$, reading as

$$\Gamma^{-1}\frac{\partial\rho(\mathbf{r},t)}{\partial t}=\nabla\cdot\left[\rho(\mathbf{r},t)\nabla\frac{\delta F[\rho(\mathbf{r},t)]}{\delta\rho(\mathbf{r},t)}\right]. \tag{5}$$

This is the central equation of DDFT. In equation (5), the equilibrium Helmholtz free energy functional is given by [17]

$$F[\rho]=\beta^{-1}\int \mathrm{d}\mathbf{r}\ \rho(\mathbf{r})\{\ln[\Lambda^3\rho(\mathbf{r})]-1\} + \int \mathrm{d}\mathbf{r}\ \rho(\mathbf{r})V_{\mathrm{ext}}(\mathbf{r},t)+F_{\mathrm{ex}}[\rho]\,, \tag{6}$$

where Λ is the (irrelevant) thermal de Broglie wavelength and $F_{\mathrm{ex}}[\rho]$ is the excess Helmholtz free energy functional, i.e. the contribution arising from interparticle interactions. Note that equation (5) has the form of a continuity equation with the current density $\mathbf{j}(\mathbf{r},t)$ given by

$$\mathbf{j}(\mathbf{r},t)\equiv-\Gamma\rho(\mathbf{r},t)\nabla\frac{\delta F[\rho(\mathbf{r},t)]}{\delta\rho(\mathbf{r},t)}\equiv-\Gamma\rho(\mathbf{r},t)\nabla\mu(\mathbf{r},t)\,, \tag{7}$$

where $\mu(\mathbf{r},t)$ is a non-equilibrium, local chemical potential that reduces to the equilibrium value in the absence of time-dependent external potentials [13]. That the DDFT equation can be written in the form of a continuity equation guarantees the conservation of the total number of particles N in the system.

Before proceeding with specific applications of DDFT, a few remarks on the issue of hydrodynamic interactions (HI) should be made. In its present formulation, HI are ignored within the DDFT. A major effect of HI can be simply incorporated by rescaling the drag coefficient Γ into an effective one [18]. With this scaling, HI can be taken into consideration in our treatment; they will just renormalize the timescale. A more detailed analysis shows that leading order corrections due to HI scale as $C^2\phi^{1/3}$, where $C=\bar{r}\phi^{1/3}/a$, $\bar{r}$ is the mean interparticle spacing, a is the physical core size, $\sigma/2$ is the interaction radius and $\phi=(4\pi/3)\rho a^3$ is the volume fraction [19–21]. In our studies (see below), we have typically $\bar{r}\approx\sigma$ and $\rho=1/\sigma^3$. Insertion yields a correction of the order of $(\sigma/2a)^2\phi=2\pi a/\sigma$. Therefore, our treatment applies to particles with small physical core size a but large interaction radius $\sigma/2$. There are several examples for such particles, e.g. stiff polyelectrolyte stars, tetrapods, star polymers and dendrimers, which fulfil these conditions.

In this work, we consider ultrasoft particles interacting by means of a bounded, Gaussian effective pair potential of the form

$$V(|\mathbf{r}-\mathbf{r}'|)=\epsilon\exp\left[-(|\mathbf{r}-\mathbf{r}'|/\sigma)^2\right]. \tag{8}$$

The Gaussian pair potential has been shown to be a realistic description for the equilibrium effective pair potentials between self-avoiding polymer coils [22], low-arm star polymers [23], dendrimers [24–26] and weakly charged polyelectrolyte chains [27]. For most cases, we set $\epsilon=k_{\mathrm{B}}T$, providing the energy unit of the system, whereas σ, which corresponds to the gyration radius of the ultrasoft particles, will be the unit of length henceforth. Accordingly, the natural timescale of the problem, providing the unit of time in this work, is the Brownian timescale τ_{B}:

$$\tau_{\mathrm{B}}=\sigma^2/(\epsilon\Gamma). \tag{9}$$

For Gaussian particles, the *mean-field* or *random-phase approximation* (RPA) functional $F_{\mathrm{ex}}[\rho]$ has been shown to be very accurate for static properties [28–35]:

$$F_{\mathrm{ex}}[\rho]=\frac{1}{2}\int\int \mathrm{d}\mathbf{r}\,\mathrm{d}\mathbf{r}'V(|\mathbf{r}-\mathbf{r}'|)\rho(\mathbf{r})\rho(\mathbf{r}'). \tag{10}$$

Inserting equations (10) and (6) into equation (5) yields

$$\begin{aligned}\Gamma^{-1}&\frac{\partial\rho(\mathbf{r},t)}{\partial t}\\ &=\beta^{-1}\nabla_{\mathbf{r}}^2\rho(\mathbf{r},t)+\nabla_{\mathbf{r}}\rho(\mathbf{r},t)\cdot\int \mathrm{d}\mathbf{r}'\ \nabla_{\mathbf{r}}V(|\mathbf{r}-\mathbf{r}'|)\rho(\mathbf{r}',t)\\ &\quad+\rho(\mathbf{r},t)\int \mathrm{d}\mathbf{r}'\ \nabla_{\mathbf{r}}^2V(|\mathbf{r}-\mathbf{r}'|)\rho(\mathbf{r}',t)\\ &\quad+\nabla_{\mathbf{r}}\rho(\mathbf{r},t)\cdot\nabla_{\mathbf{r}}V_{\mathrm{ext}}(\mathbf{r},t)+\rho(\mathbf{r},t)\nabla_{\mathbf{r}}^2V_{\mathrm{ext}}(\mathbf{r},t).\end{aligned} \tag{11}$$

Given an initial density field $\rho(\mathbf{r},t=0)$ and a prescribed external potential $V_{\mathrm{ext}}(\mathbf{r},t)$, equation (11) can be solved numerically to obtain $\rho(\mathbf{r},t)$. We have considered external potentials that are either spherically symmetric, $V_{\mathrm{ext}}(\mathbf{r},t)=V_{\mathrm{ext}}(r,t)$ or depend on a single Cartesian coordinate, $V_{\mathrm{ext}}(\mathbf{r},t)=V_{\mathrm{ext}}(z,t)$. In these cases the resulting density is a function of r, $\rho(\mathbf{r},t)=\rho(r,t)$, and of z, $\rho(\mathbf{r},t)=\rho(z,t)$, respectively.

2.2. *Numerical details*

The partial differential equation governing the time evolution of $\rho(\mathbf{r},t)$, equation (11), was solved numerically employing the Forward Time Centred

Space (FTSC) algorithm [36]. This method employs a finite difference approximation to solve the initial value problem and requires appropriate boundary conditions. We have discretized the density on a grid with spacing Δr for the spherically symmetric external potentials and Δz for the planar ones, using $\Delta r = \Delta z = 0.001\,\sigma$. For the case of spherical confinement, the maximum distance $r_{\max}$ was chosen to be four to five times the extension of the confining cavity, thus the density field could be set to zero at the system's boundaries, without imposing any artefacts. Since the applied difference scheme is only accurate to the first order in Δt, we use a small time step $\Delta t = 10^{-6}\tau_{\mathrm{B}}$ in solving equation (11), to guarantee sufficient accuracy.

In order to check the accuracy of the approximate DDFT equation (5), we have accompanied our study with Brownian dynamics (BD) simulations of the original Langevin equations (equation (1)) that describe the microscopic dynamics of the fluid. For the cases in which the external potential depends only on one spatial coordinate, z, we fix the value of the density per unit area $\rho_0 = \int \mathrm{d}z\rho(z,t)$. The Langevin equations of motion including the external field are numerically solved using a finite time step $\Delta t = 0.002\tau_{\mathrm{B}}$ in all simulations, together with the technique of Ermak [37, 38]. In order to obtain the time-dependent density $\rho(\mathbf{r},t)$ we perform a large number N_{run} of independent runs with different initial configurations, typically $N_{\mathrm{run}} = 5000$, sampled from a situation with a static external potential. We checked that after a sufficiently long time of roughly $t = 5\tau_B$, the system runs into the same steady-state for all initial configurations chosen.

3. Time-varying external fields

In this section we consider a system of particles interacting by means of the Gaussian potential of equation (8) in time-varying, spherically symmetric geometric confinements. The energy scale ϵ in equation (8) has the value $\epsilon = k_{\mathrm{B}}T$. An additional parameter is the total number of particles, $N = \int \mathrm{d}\mathbf{r}\rho(r,t)$. Since this is a conserved quantity, it is sufficient to fix its value at $t = 0$. We have chosen $N = 100$ throughout.

3.1. *Cavities of oscillating size*

We first examine the Gaussian fluid in an explicitly time-dependent, radially symmetric external potential that is periodic in time and is described by

$$V_{\mathrm{ext}}(r,t) = \Phi_0\big[(r/R_1)^{10}\Theta(-\sin(2\pi t/\tau)) + (r/R_2)^{10}\Theta(\sin(2\pi t/\tau))\big]\,, \qquad (12)$$

where $r = |\mathbf{r}|$, $R_1 \neq R_2$ are two distinct length scales, Φ_0 sets the strength of the external potential, $\Theta(x)$ is the Heaviside function, which is defined as follows

$$\Theta(x) = \begin{cases} 1\,, & \text{if } x \geq 0\,; \\ 0\,, & \text{if } x < 0\,, \end{cases} \qquad (13)$$

and τ is the period of the change of the external potential. This potential models a spherical confining cavity with a sudden, periodically repeating change in size between R_1 and R_2. Henceforth, we will refer to R as the length scale of the cavity. Every $\tau/2$ the length scale jumps suddenly from R_1 to R_2 and vice versa. After each change in R, the system tries to relax to its equilibrium configuration determined by the new length scale, until the size of the cavity changes again. Hence, depending on the period τ, full relaxation to equilibrium is hindered by the constant 'kicks' from the external potential and the system rather reaches a steady-state, periodically repeating density profile $\rho(r,t) = \rho(r,t+\tau)$.

We choose $\Phi_0 = 10k_{\mathrm{B}}T$, $R_1 = 5\sigma$ and $R_2 = 4\sigma$. Previous work on this system has already been carried out by Dzubiella and Likos [9], who examined the relaxation of the density profiles under a single sudden expansion or compression. In this work, the expansion and compression processes alternate and repeat themselves periodically, as is evident from the form of the potential described by equation (12). In [9], it was found that the system exhibits three characteristic timescales. One timescale, $\tau^+ = 0.287\tau_{\mathrm{B}}$ characterizes the expansion process, whereas two distinct scales, $\tau_1^- = 0.036\tau_{\mathrm{B}}$ and $\tau_2^- = 0.189\tau_{\mathrm{B}}$ show up during the compression process [9]. Whereas τ^+ is a characteristic relaxation time for the expansion, the compression is, in fact, a two-step process: upon a sudden shrinking of the confining potential, first a fast process, characterized by the timescale τ_1^-, takes place, in which the fluid is confined in the new cavity but still far from equilibrium. Thereafter, a slower relaxation to equilibrium takes place, with a characteristic time τ_2^-.

Motivated by knowledge of these timescales, we examine the steady-state response of the system for four different choices of the period τ, namely $\tau_{1,2} = 2\tau_{1,2}^-$ and $\tau_3 = 2\tau^+$, as well as for the period $\tau_4 = 2\tau_{\mathrm{B}}$. In figure 1 we display the density profiles at the steady state, taken at the moment exactly before the cavity changes its radius from R_1 to R_2 or vice versa. In other words, the system has just spent a time interval $\Delta t_i = \tau_i/2$ $(i = 1,2,3,4)$ in a cavity of the size indicated on the plots.

We observe excellent agreement between the BD simulation results and those from DDFT, in all cases considered. The timescale τ_4 is sufficiently long that

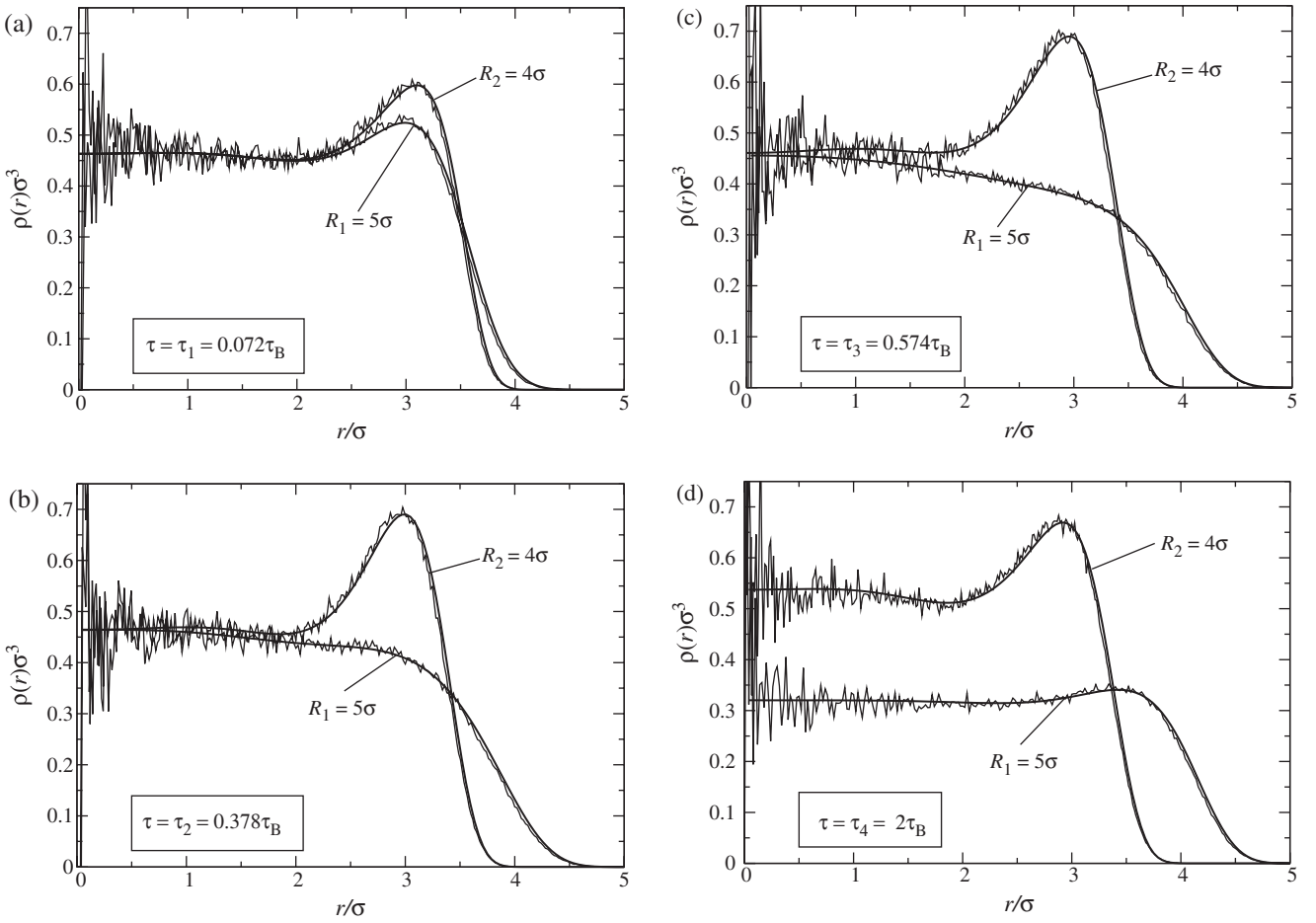

Figure 1. DDFT (solid curves) and BD results (noisy lines) of the *steady-state* density profiles $\rho(r, t)$ under the influence of the external potential of equation (12) for four different choices of the period τ: (*a*) $\tau = \tau_1 = 2\tau_1^- = 0.072\tau_B$; (*b*) $\tau = \tau_2 = 2\tau_2^- = 0.378\tau_B$; (*c*) $\tau = \tau_3 = 2\tau^+ = 0.574\tau_B$ and (*d*) $\tau = \tau_4 = 2\tau_B$. In all cases, $\Phi_0 = 10k_BT$, $R_1 = 4\sigma$ and $R_2 = 5\sigma$.

at the end of every half-period the system reaches the profile corresponding to static equilibrium for the corresponding value $R_{1,2}$; the profiles are depicted in figure 1 (*d*). If on the other hand, the period of switching is much shorter the density profiles barely change, since the system has no time to react to the rapidly changing external field. Such a case is displayed in figure 1 (*a*), corresponding to $\tau = \tau_1$. The density profiles only change close to the cavity boundaries and remain unaffected by the switching of the external field towards its centre. This situation persists for the cases where $\tau = \tau_2$ and $\tau = \tau_3$ shown in figures 1 (*b*) and (*c*). It is mainly the outer part of the density profile that experiences the influence of the time-varying external field, leading also to an overshoot of the larger density peak over its equilibrium height, as the cavity size shrinks, an effect observed also in the case of a single compression process [9].

In order to analyse the time dependence of the density fields more quantitatively, we introduce the second moment of the density, $m_2(t)$, defined as

$$m_2(t) = \int \mathrm{d}\mathbf{r} r^2 \rho(r, t). \tag{14}$$

Clearly, $m_2(t)$ is a measure for the spread of the density around the centre of the external potential at any given time t. In figure 2 we display a representative result for $m_2(t)$ for the period τ_1, as obtained by solving the DDFT equation. Evidently, the system needs several periods until it reaches the steady-state, periodic solution. Moreover, we define the squared amplitude, $A^2(\tau)$, of the oscillations as the difference between the maximum and minimum values of $m_2(t)$ in the steady state:

$$A^2(\tau) = \max\{m_2(t)\} - \min\{m_2(t)\}. \tag{15}$$

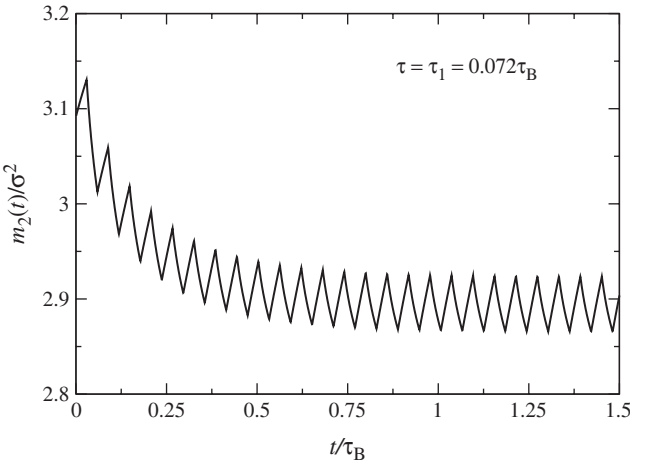

Figure 2. The second moment of the radial density profile, $m_2(t)$, as defined in equation (14), against the time t as obtained by DDFT. The external potential is that of equation (12) and the period is $\tau_1 = 0.072\tau_B$.

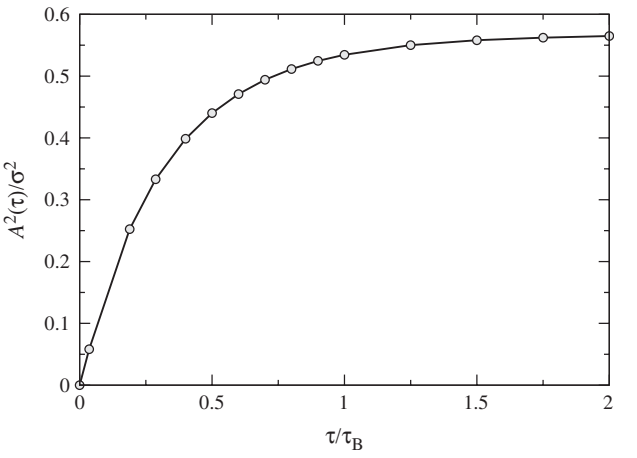

Figure 3. The squared amplitude $A^2(\tau)$, as defined in equation (15), for the system of Gaussian particles in the time-varying spherical confining potential of equation (12), against the switching period τ of the latter. The line is simply connecting points at which the amplitude was calculated, which are denoted by the grey circles.

Since the response of the system depends on the period of the external field, the amplitude becomes a function of τ.

In figure 3 we show the dependence of $A^2(\tau)$ on τ. For sufficiently long periods, $\tau \gtrsim \tau_B$, the squared amplitude $A^2(\tau)$ approaches a constant value, which is due to the fact that the system relaxes completely into its equilibrium configuration within a half-period. For small τ the amplitude goes to zero, because the changes in the external potential occur on timescales much shorter than the Brownian timescale and are therefore too fast for the particles to follow. We find no resonant response of the system (maximum of $A^2(\tau)$ for some specific period) but rather a monotonic dependence of the amplitude on τ. This can be understood in terms of the overdamped nature of the dynamics. It is a well known fact that, for instance, the Brownian harmonic oscillator in the absence of the stochastic force does not not exhibit a resonant frequency either. This behaviour can be generalized to our problem.

Whereas the external potential of equation (12) does feature a periodic time dependence, it has the particularity that it is time-independent throughout a whole half-period $\tau/2$, i.e. the changes of the external potential are instantaneous. We now proceed to examine a more involved case, in which the external potential $V_{ext}(r, t)$ changes continuously with time. We confine the system inside a spherical cavity whose effective radius is changing with time in a sinusoidal fashion and modelled by the external potential

$$V_{ext}(r, t) = \Phi_0 \left[\frac{r}{(R + a \sin(2\pi t/\tau))} \right]^{10}, \qquad (16)$$

where Φ_0 again sets the strength of the potential, R is the cavity radius, and τ and a are the period and the amplitude of the radius oscillations, respectively. Thus, the instantaneous size of the cavity, $R(t) = R + a \sin(2\pi t/\tau)$, oscillates between $R \pm a$ with a period τ. We choose the parameters as $\Phi_0 = 10 k_B T$, $R = 5\sigma$ and $a = \sigma$. Here, we have a fully time-dependent external potential and therefore the possibility of studying fully-developed as opposed to relaxation dynamics.

In figure 4 we show the steady-state solutions of the density profile for four different choices of the oscillation period, $\tau_1 = 0.1\tau_B$, $\tau_2 = 0.4\tau_B$, $\tau_3 = \tau_B$ and $\tau_4 = 2\tau_B$. Once more, excellent agreement between the DDFT and Brownian Dynamics simulations is found, demonstrating thus the ability of the former to capture the full dynamics of a system of overdamped particles. Some of the features that we found in the previous section are also seen here. As for the case of the external potential of equation (12), we find that for small periods, such as τ_1 and τ_2, figures 4 (*a*) and (*b*), the centre of the system is hardly influenced by the changes in the external potential. At the same time, there are also important differences between the response of the system to sudden or continuous changes of the external potential. For the longest period, $\tau_4 = 2\tau_B$, for which the density profiles are shown in figure 4 (*d*), we can ascertain that the system is still quite far from the quasistatic response, i.e. the density profile at any time is *not* identical with the equilibrium profile for the instantaneous value of the cavity's radius. Here, the profiles for $R = 5\sigma$ differ, depending on whether this

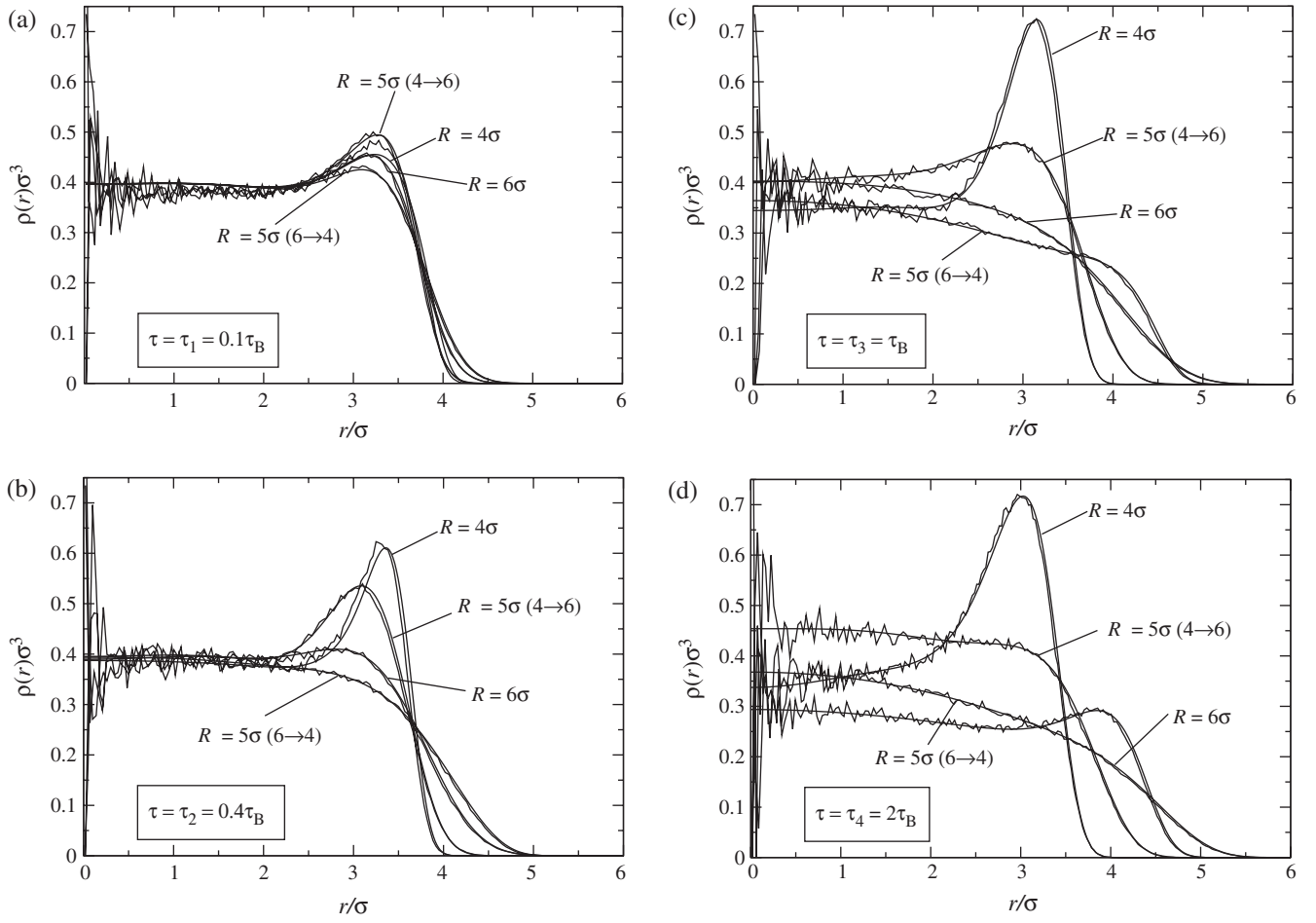

Figure 4. DDFT (solid curves) and BD results (noisy lines) of the *steady-state* density profiles $\rho(r, t)$ under the influence of the external potential of equation (16) for different periods τ: (*a*) $\tau = \tau_1 = 0.1\tau_B$; (*b*) $\tau = \tau_2 = 0.4\tau_B$; (*c*) $\tau = \tau_3 = \tau_B$ and (*d*) $\tau = \tau_4 = 2\tau_B$. The parameters of the external potential read $\Phi_0 = 10k_BT$, $R_0 = 5\sigma$ and $a = \sigma$. The labels on the plots denote the instantaneous value of the cavity radius. As the instantaneous value $R(t) = 5\sigma$ is reached twice within a period cycle, the numbers in the parentheses indicate whether this value occurs during the 'expansion' ($4 \to 6$) or the 'compression' ($6 \to 4$) stage of the oscillation.

value of the radius is reached during the expansion ($4 \to 6$) or compression ($6 \to 4$) half-cycle, as indicated by the numbers in the brackets in figure 4. This should be contrasted with the case in figure 1(*d*), which pertains to the density profiles under the influence of external potential equation (12). In this case, a switching period $\tau = 2\tau_B$ is long enough for the system to react in a quasistatic fashion. Evidently, the continuous change of external potential equation (16) prevents the system from exhibiting a quasistatic response for τ that largely exceed those relevant for external potential (12), which features only sudden changes. We find that a quasistatic response to external potential (16) occurs only for very large values of the period, $\tau_s \gtrsim 250\tau_B$. In figure 5 we display the steady-state density profiles, where it can be seen that the profile for $R(t) = 5\sigma$ is independent of whether the instantaneous value of the confining radius is reached during compression or expansion.

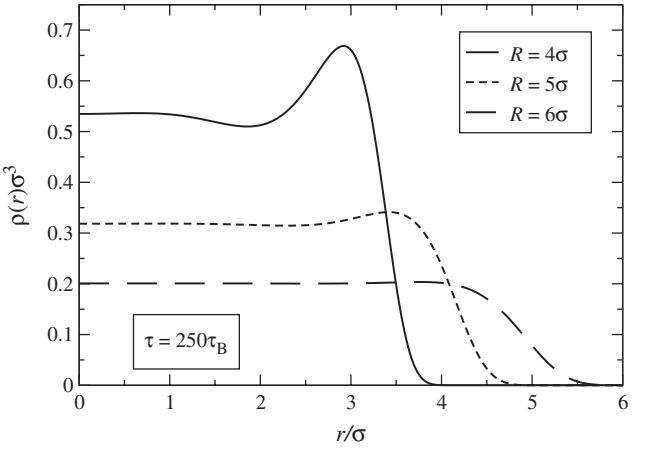

Figure 5. DDFT results of the *steady-state* density profiles $\rho(r, t)$ under the influence of the external potential (16) for the period $\tau = 250\tau_B$ and for $\Phi_0 = 10k_BT$, $a = \sigma$ and $R = 5\sigma$. Here, the time evolution of the system is quasistatic.

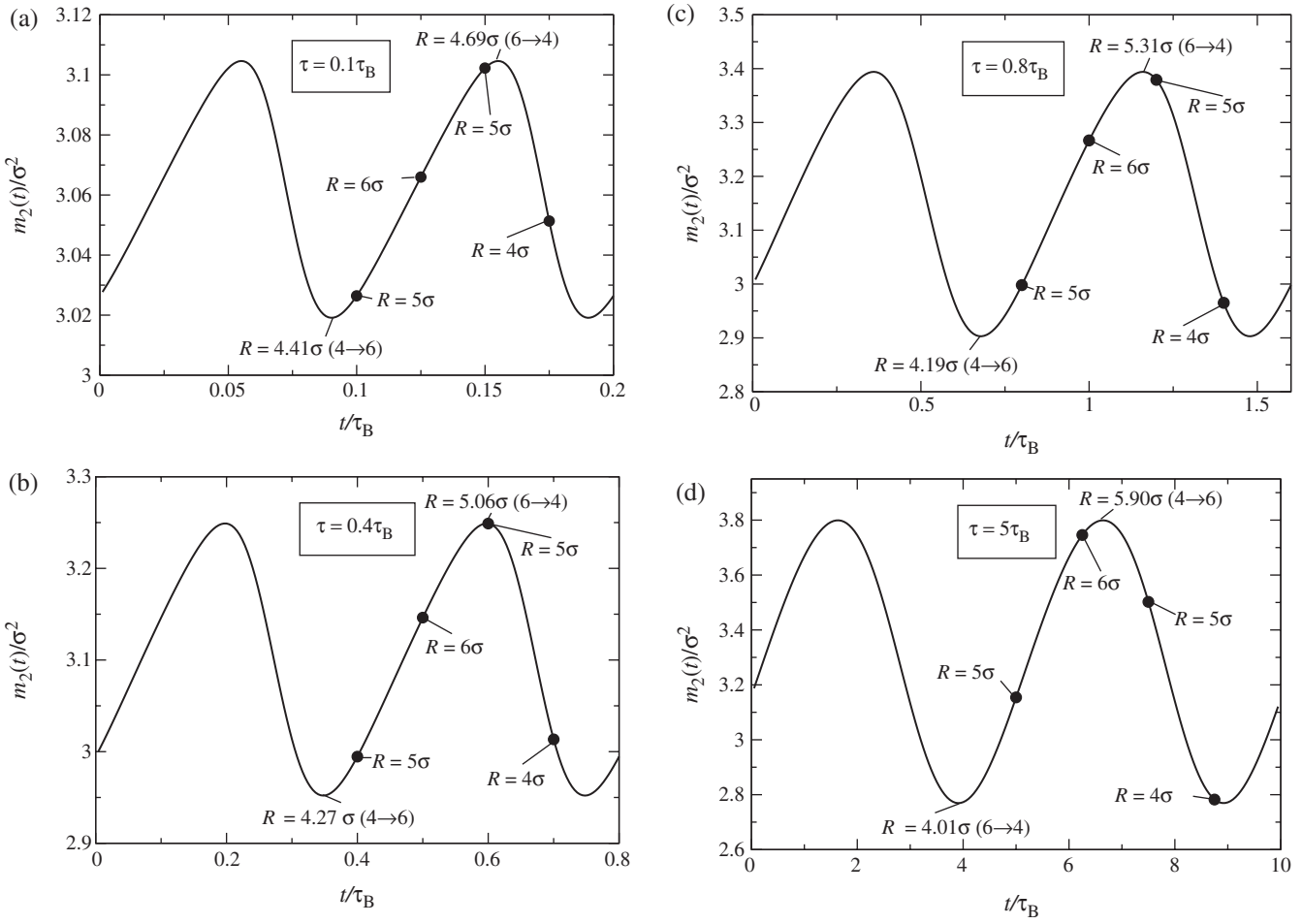

Figure 6. The second moment of the radial density profile, $m_2(t)$, defined in equation (14) plotted against time t for the spherical external potential equation (16) for the periodic times: (*a*) $\tau = 0.1\tau_B$; (*b*) $\tau = 0.4\tau_B$; (*c*) $\tau = 0.8\tau_B$ and (*d*) $\tau = 5\tau_B$. The labels on the plots indicate the instantaneous values of the cavity radius and the numbers in the parentheses have the same meaning as in figure 4. The dots indicate the time after each quarter of the periodic time for which the instantaneous values of the cavity radius are displayed in the plot as well.

On the other hand, for $\tau \lesssim \tau_s$, we find a depleted zone at the outermost parts of the density profile for $R = 6\sigma$, when compared with the static equilibrium density profile; the oscillations are too fast for particles to reach this region. In summary, a cavity with a sinusoidally oscillating radius requires an enormous increase of the timescale necessary for the system to reach quasistatic response, whereas for a sudden, periodically oscillating radius, this occurs for periods exceeding, roughly, $2\tau_B$. In the case of continuous oscillations this threshold value increases by two orders of magnitude.

Additionally, we find that there is a phase-shift φ between the external potential and the response of the system. For sufficiently rapid oscillations, $\tau = \tau_1$, shown in figure 4 (*a*), both the maximum value of $\rho(r)$ and its maximum extension in r are achieved for $R = 5\sigma$, the former during the expansion and the latter during the compression processes of the oscillation. These are purely dynamical effects, since in the static case the density peak is highest for the most confined cavity ($R = 4\sigma$) and its extension is maximal for the most expanded cavity ($R = 6\sigma$). Upon increasing the oscillation period, the maximal density peak appears indeed for $R = 4\sigma$, as seen in figures 4 (*b*)–(*d*). This is what one would intuitively expect, since the equilibrium profile is maximal for $R = 4\sigma$ among the radii we considered, see figure 5.

For a more quantitative analysis, we again look at the second moment of the density, $m_2(t)$, defined in equation (14) above. This quantity is shown in figure 6 for four different oscillation periods, $\tau = 0.1\tau_B$, $\tau = 0.4\tau_B$, $\tau = 0.8\tau_B$ and $\tau = 5\tau_B$. For $\tau = 0.1\tau_B$, figure 6 (*a*), the periodic maxima and minima of $m_2(t)$

occur for the instantaneous cavity radius $R = 4.41\sigma$ and $R = 4.69\sigma$, during the compression and expansion phases, respectively. This is already counterintuitive, since, from the static point of view, compression *shrinks* the system and expansion *swells* it, hence one would expect that $m_2(t)$ is smaller in the former than in the latter case. This ordering of maxima and minima persists also to the longer period, $\tau = 0.4\tau_B$, shown in figure 6 (*b*). The maximum of $m_2(t)$, at $R = 5.06\sigma$, is still far from its expected instantaneous cavity radius $R = 6\sigma$ from static considerations. Upon further slowing down the frequency of oscillations, $\tau = 0.8\tau_B$, shown in figure 6 (*c*), the minimum of $m_2(t)$ occurs for $R = 4.19\sigma$, which is already close to the most compressed state, $R = 4\sigma$, while the maximum remains far from $R = 6\sigma$; the instantaneous radius value is $R = 5.31\sigma$ during the compression process. At the even slower frequency, $\tau = 5\tau_B$, shown in figure 6 (*d*), the maxima and minima of $m_2(t)$ approach the expectations arising from static considerations, yet the system is still far from quasistatic evolution.

The extensions of the cavity for which $m_2(t)$ are minimal and maximal are thus continuous functions of the period τ or, in other words, the phase shift φ between the external potential and the response of the system is a continuous function of the frequency $\omega = 2\pi/\tau$. In the quasistatic case, the system and the external potential have to be in phase, whereas the phase shift increases with increasing frequencies. This effect stems from the Brownian nature of the dynamics.

To gain some insight into the physical origin of the frequency-dependent phase shift, we put forward here a simple physical picture. We consider a random colloidal particle with instantaneous position coordinate $x(t)$, taking one-dimensional motion for simplicity. The remaining particles provide a restoring force $-Cx(t)$ around the particle's local equilibrium position, whereas the solvent acts on it by inducing a friction contribution $-b\dot{x}(t)$. An additional, external force $F(t) = F_0 \cos(\omega t)$, stemming from the oscillating external potential, is also acting on the particle. In the spirit of the Langevin equations (1), we ignore the inertial contributions to the equations of motion (overdamped case) and thus $x(t)$ obeys the first-order differential equation:

$$b\dot{x}(t) + Cx(t) = F_0 \cos(\omega t). \tag{17}$$

Defining $\Gamma \equiv 1/b$, equation (17) takes the form

$$\dot{x}(t) = -\Gamma[Cx(t) - F_0 \cos(\omega t)]. \tag{18}$$

Equation (18) above is analogous to the coupled Langevin equations (1). The absence of the random force contributions at the right-hand side of equation (18) does not affect the arguments to follow, which pertain to the ω-dependence of the particle's response. Equation (18) can be solved using standard methods, yielding the solution $x(t) = x_0 \cos(\omega t + \varphi)$, with the amplitude x_0 and the phase shift φ given by

$$x_0 = \frac{F_0}{C} \frac{\Gamma C}{[(\Gamma C)^2 + \omega^2]^{1/2}} \tag{19}$$

and

$$\varphi = -\tan^{-1}\left(\frac{\omega}{\Gamma C}\right). \tag{20}$$

The amplitude of the oscillation, x_0, attains its maximum as $\omega \to 0$, decreasing monotonically thereafter as ω grows. In the same limit, the phase difference φ approaches zero, thus the system and the external stimulus oscillate in phase. In the opposite limit, $\omega \to \infty$, the phase difference between the external force and the particle's response tends to the limiting value $\varphi_\infty = -\pi/2$. Moreover, the amplitude x_0 becomes vanishingly small, precisely as seen in our many-body system as well.

We now examine the frequency-dependent squared amplitude of the system's response, $A^2(\tau)$, defined in equation (15) for the case with external potential (12). In order to explore the limits of the analogy with the driven, overdamped harmonic oscillator described above, we have attempted to fit our results with a functional form inspired by the τ-dependence of the one-particle analogue of $A^2(\tau)$, namely the quantity x_0^2. Following equation (19), and setting $\tau/\tau_B \equiv \xi$, we propose to describe the τ-dependence of $A^2(\tau)$ through the two-parameter fit function:

$$f(\xi) = \frac{\alpha_0}{1 + \alpha_1 \xi^{-2}}\ , \tag{21}$$

where the two parameters, α_0 and α_1, play a role analogous to the single-particle quantities F_0/C and $(\Gamma C)^{-1}$, respectively. The raw DDFT data and the best χ^2-fit, achieved for $\alpha_0 = 0.458$ and $\alpha_1 = 0.131$, are shown in figure 7. It can be seen that the results can indeed be very well described by the functional form (21), demonstrating that the analogy between the many-body system and a single, driven, Brownian oscillator can be carried to a quantitative level. This is an intriguing result, in view of the complexity of the interacting system and the simplicity of its one-particle counterpart.

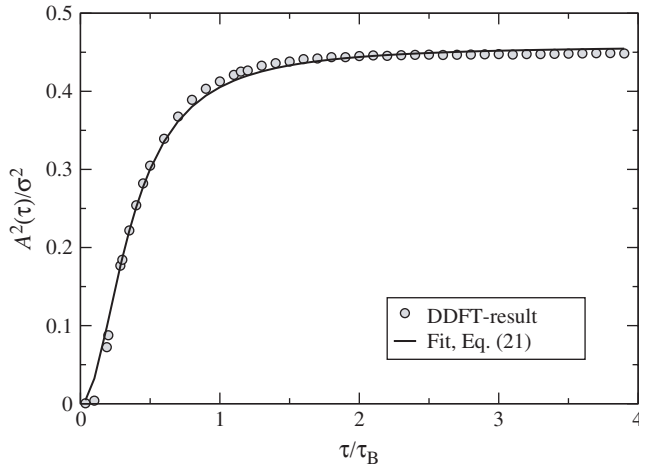

Figure 7. The squared amplitude $A^2(\tau)$ for the density profiles under the influence of the external potential of equation (16) versus the period τ of the latter. The grey circles are the DDFT results and the solid line is the best fit obtained by using a functional form given by equation (21).

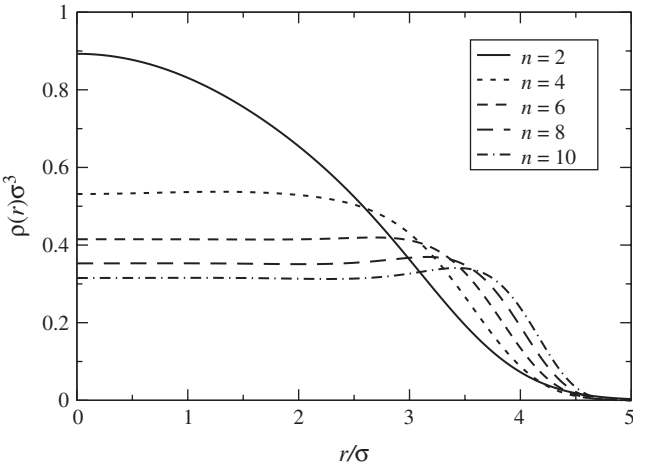

Figure 8. The equilibrium density profiles of the ultrasoft, Gaussian colloids ($N = 100$ particles) for different exponents n in the external potential of equation (22). The values of the exponents are indicated in the legend.

3.2. *Cavities of oscillating sharpness*

In both the preceding cases with time-dependent potentials, given by equations (12) and (16), we have seen that the external influences have chiefly influenced the parts of the density profile lying close to the cavity borders, i.e. for $r \cong R$. In the next example, we examine how one can directly influence the density field in the *centre* of a spherical cavity by introducing an external potential of oscillating *sharpness*. This is achieved by temporally modulating the exponent n, namely:

$$V_{\text{ext}}(r, t) = \Phi_0 (r/R)^{n(t)} , \tag{22}$$

where Φ_0 is the strength of the potential and

$$n(t) = n_0 + m \sin(2\pi t/\tau). \tag{23}$$

The exponent n oscillates around n_0 with period τ and amplitude m. The external potential of equations (22) and (23) represents a spherical cavity of fixed size R but with the sharpness of the confinement changing continuously with time t. We choose the parameters $\Phi_0 = 10 k_B T$, $n_0 = 6$ and $m = 4$. The equilibrium density profiles of this system for several exponents n are shown in figure 8.

It is evident that potential equation (22) is capable of influencing the centre rather than the outer parts of the system. In figure 9 we display DDFT and simulation results for the steady-state density profiles for various choices of the period τ. Once again, we find excellent agreement between theory and simulation. The centre of the fluid is mainly influenced, as expected, whereas the outer parts of the system remain relatively untouched. Thereby, the system can be manipulated selectively at its centre (by employing external potentials of the current form) or at its periphery (by using external potentials of oscillating size). As before, we find that for sufficiently rapid changes in the external potential, the system hardly responds, see figure 9 (*a*). Moreover, even for the long oscillation period $\tau_4 = 2\tau_B$, the system is still far from showing quasistatic evolution.

Just as for the case with external potential given by equation (16), we find a phase shift φ between the external potential and the response of the system, which depends on the periodic time τ. In order to quantify this shift, we focus now on the quantity that responds most sensitively to the external field, namely the value of the density profile at the origin, $\rho(r = 0, t)$. Representative results for two choices of the period τ are shown in figure 10. Whereas in the static case this quantity has a maximum for $n = 2$ and a minimum for $n = 10$ (see figure 8), in the dynamical case the positions of the extrema are shifted. For rapid oscillations, figure 10 (*a*), the effect is more drastic than for slower ones, figure 10 (*b*). Moreover, the amplitude of the oscillations in $\rho(r = 0, t)$ increases as the frequency decreases, in full analogy with the previously found results.

4. Layer diffusion

In this section, we examine an even more drastic inhomogeneity. We start from an external potential that creates a layer of particles which is well separated from the rest. By suddenly switching this potential to

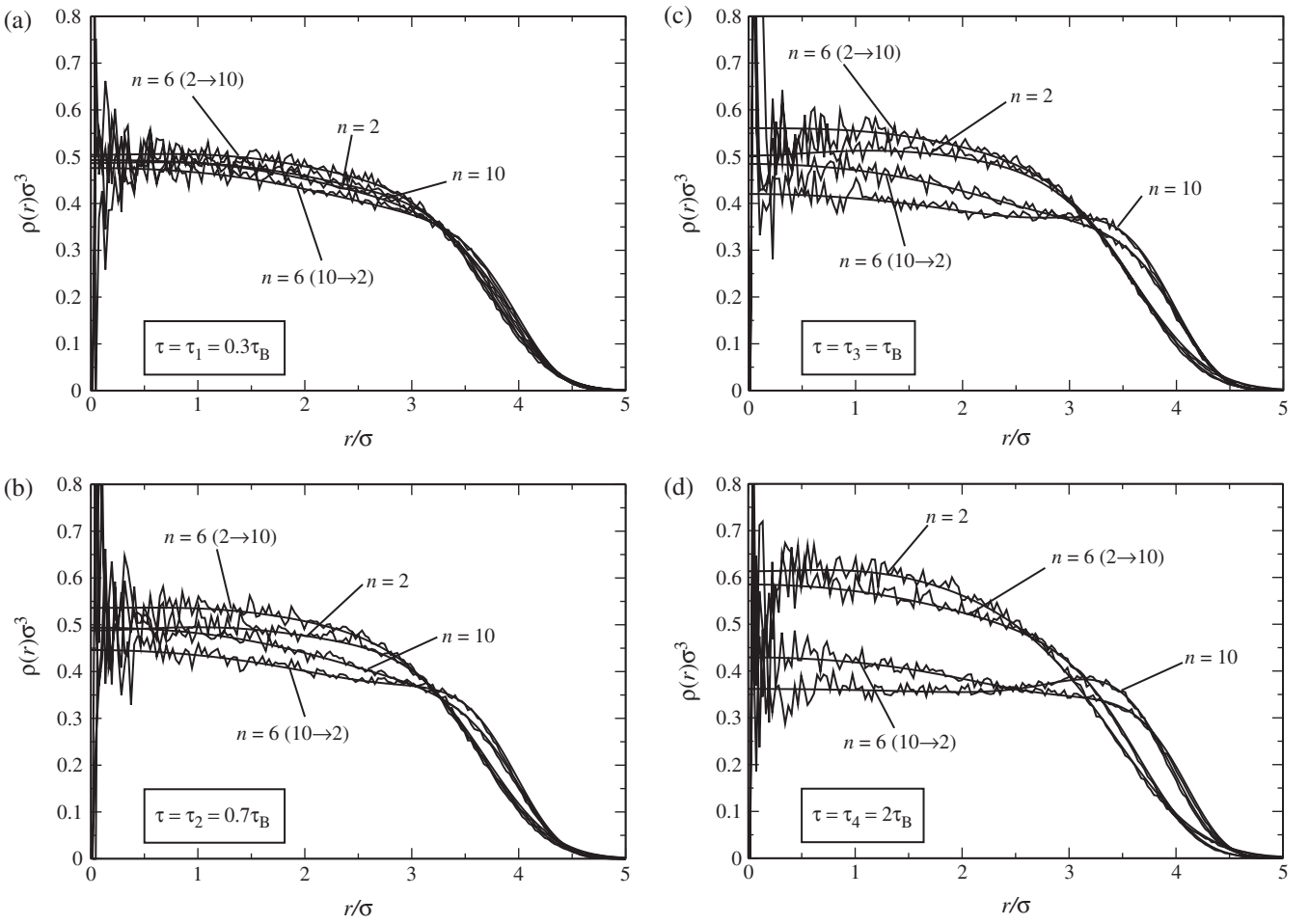

Figure 9. DDFT (straight curves) and BD results (noisy curves) of the *steady-state* density profiles $\rho(r, t)$ under the influence of the external potential of equation (22) for periods: (*a*) $\tau = \tau_1 = 0.3\tau_B$; (*b*) $\tau = \tau_2 = 0.7\tau_B$; (*c*) $\tau = \tau_3 = \tau_B$ and (*d*) $\tau = \tau_4 = 2\tau_B$. The remaining parameters have the values $\Phi_0 = 10k_BT$, $n_0 = 6$ and $m = 4$. The labels on the plots indicate the instantaneous values of the exponent and the numbers in the parentheses have the same meaning as in figure 4.

zero the layer diffuses and the system relaxes back to the constant equilibrium density. We show that even for this very strong inhomogeneity which resembles a crystalline structure the DDFT reproduces almost perfectly the results of the Brownian dynamics simulations.

The external model potential which creates the particle layer reads as

$$V_{\text{ext}}(z, t) = \Phi_0\{\exp[-10(\bar{z} - 1)^2] + \exp[-10(\bar{z} + 1)^2]\}\Theta(-t)\,, \qquad (24)$$

where $\bar{z} \equiv z/\sigma$ and $\Phi_0 = 10k_BT$ sets the strength of the potential. As the external potential depends only on one spatial coordinate z, we have $\rho(\mathbf{r}, t) = \rho(z, t)$. It is supposed that the external potential of equation (24) has acted on the system sufficiently long ($t < 0$), so that thermodynamic equilibrium has been reached at $t = 0$. Then, for $t > 0$, the constraint is switched off and the previously confined layer is allowed to diffuse into the rest of the system, restoring an overall uniform density profile. We considered two cases of interaction strengths between the particles (equation (8)), $\epsilon = k_BT$ as well as $\epsilon = 10k_BT$. The higher interaction strength results in stronger correlations between the particles and thus allows us to put the theory to a more stringent test.

In figure 11 we show a simulation snapshot of the particles' positions before lifting off the external potential. We checked that the density between the layer and the remaining system is zero within the numerical accuracy, to verify that the layer is almost completely separated from the system.

The results of the DDFT and the Brownian Dynamics simulations are shown in figure 12 (*a*) for interaction strength between the Gaussian particles $\epsilon = 1k_BT$ and in figure 12 (*b*) for $\epsilon = 10k_BT$. Whereas in figure 12 (*a*) we see a single peak at $z = 0$ initially, in figure 12 (*b*) there is a double peak at, roughly, $z = \pm\sigma/2$. The reason

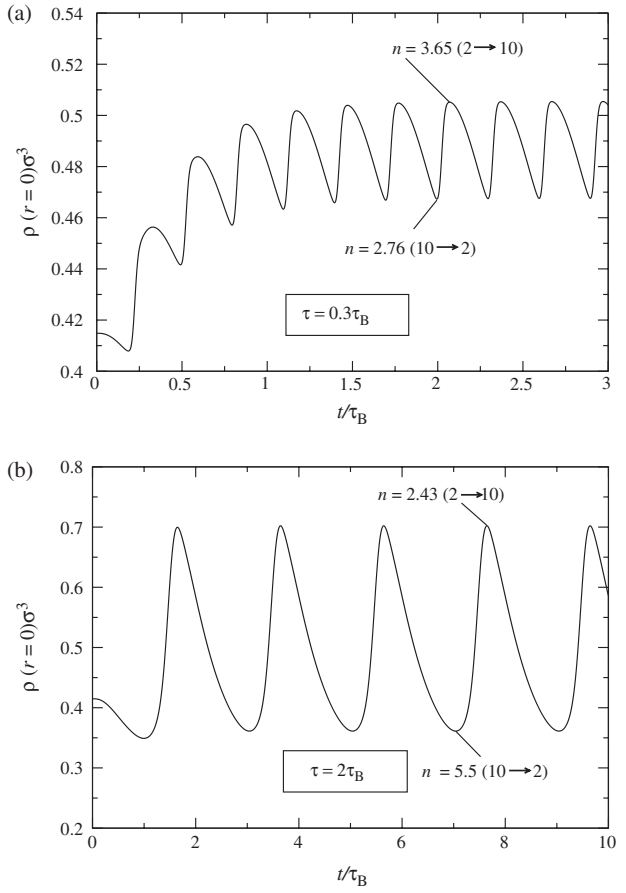

Figure 10. DDFT results of the *steady-state* density value $\rho(r=0,t)$ under the influence of the external potential of equation (22) for the periods: (*a*) $\tau=\tau_1=0.3\tau_B$ and (*b*) $\tau=\tau_4=2\tau_B$.

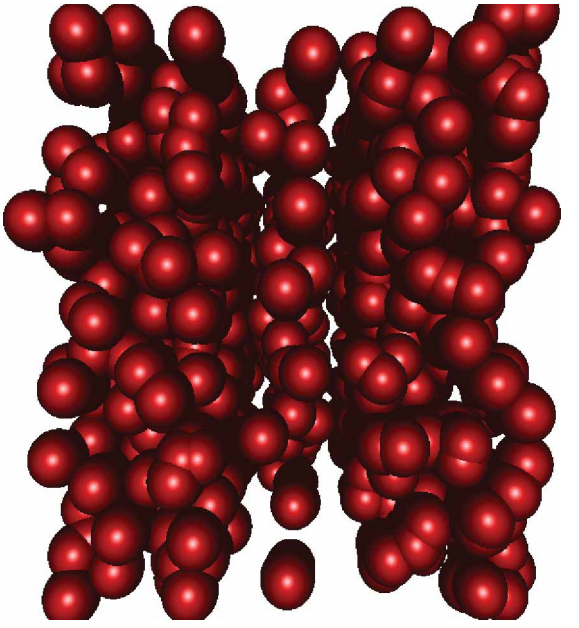

Figure 11. Simulation snapshot of a layer of particles that is separated from the rest of the system via the external potential equation (24). Here, $\epsilon=10k_BT$.

lies in the much stronger interparticle repulsion in case (*b*), which causes a 'splitting' into two sublayers within the confined layer, see also the simulation snapshot in figure 11.

As can be seen in figure 12, the DDFT equation (5) describes quite accurately also the diffusion of single layers into the bulk and the subsequent relaxation of the density into its homogeneous, bulk value. Hence one may conclude that DDFT works also in strongly inhomogeneous situations and it can be expected that freezing, melting and crystal nucleation can be tackled within DDFT.

5. Summary and concluding remarks

We have applied the dynamical density functional theory of Marconi and Tarazona [5] to examine the full dynamics of a collection of ultrasoft, Gaussian particles in a variety of spatially and temporally varying, external confining fields. We employed a very accurate yet remarkably simple static density functional [28–30] for the ultrasoft colloids and we found excellent agreement between theory and simulation in all cases considered. We analysed quantitatively the response of concentrated systems under the influence of oscillating external fields, drawing quantitative analogies with the problem of a periodically driven Brownian harmonic oscillator. In a different problem, we established that DDFT describes strong inhomogeneities very accurately by investigating the diffusion of an initially confined layer of Gaussian particles. This offers confidence that DDFT will be capable of describing other problems in which strong inhomogeneities are present such as, e.g. nucleation in supercooled fluids.

The dynamical density functional theory of Marconi and Tarazona therefore provides an excellent theoretical tool for the study of the dynamics of colloids under arbitrary external fields. However, it must be emphasized that since the theory rests on an accurate description of the statics, employment of a reliable equilibrium density functional is essential to its success. The theory can be hence applied to a variety of dynamical problems, e.g. dynamics of sedimentation, pattern formation in driven systems, microfluidics etc. A major challenge remaining for future consideration is the incorporation of hydrodynamic interactions into the theoretical formalism, either in a microscopic or in a phenomenological fashion.

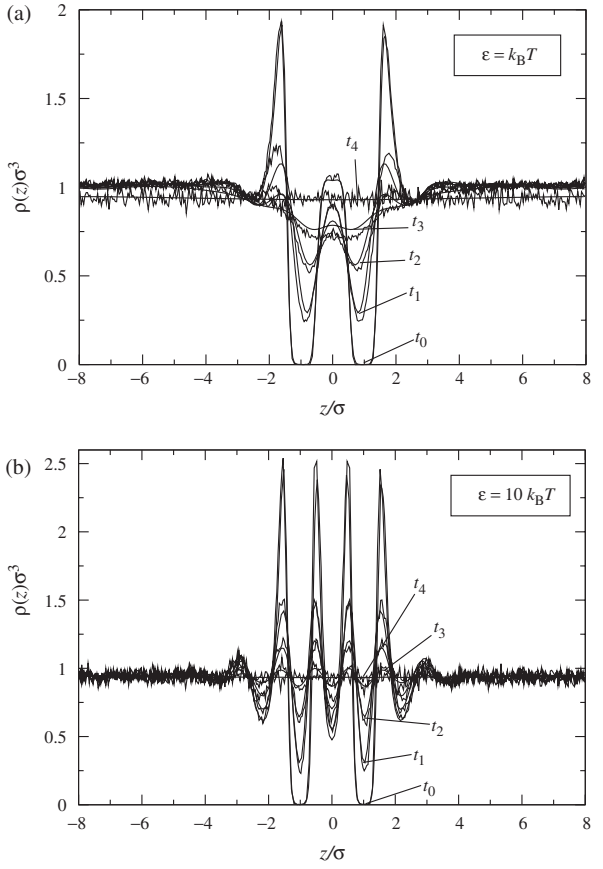

Figure 12. DDFT (straight curves) and BD results (noisy curves) of the density profiles $\rho(z, t)$. The initial density is determined by the external potential equation (24). Shown are the results for two different interaction strengths of the Gaussian interparticle potential $V(|\mathbf{r} - \mathbf{r}'|)$: (*a*) $\epsilon = k_B T$ and (*b*) $\epsilon = 10 k_B T$. The times are: (*a*) $t_0 = 0$, $t_1 = 0.05\tau_B$, $t_2 = 0.1\tau_B$, $t_3 = 0.2\tau_B$, $t_4 = 2\tau_B$; (*b*) $t_0 = 0$, $t_1 = 0.2\tau_B$, $t_2 = 0.5\tau_B$, $t_3 = \tau_B$, $t_4 = 2\tau_B$.

Acknowledgements

The authors thank Andrew Archer (University of Bristol) for a critical reading of the manuscript. This work has been supported by the Deutsche Forschungsgemeinschaft (DFG) through the Collaborative Research Centre SFB-TR6, 'Physics of Colloidal Dispersions in External Fields', Project Section C3.

References

[1] R. Evans, Adv. Phys. **28,** 143 (1979); see also R. Evans. in *Fundamentals of Inhomogeneous Fluids*, edited by D. Henderson (Dekker, New York, 1992), chap. 3.
[2] T. Munakata, Phys. Rev. E **50,** 2347 (1994).
[3] J. Araki and T. Munakata, Phys. Rev. E **52,** 2577 (1995).
[4] D. S. Dean, J. Phys. A **29,** L613 (1996).
[5] U. Marini Bettolo Marconi, and P. Tarazona, J. Chem. Phys. **110,** 8032 (1999).
[6] A. J. Archer and M. Rauscher, J. Phys. A: Math. Gen. **37,** 9325 (2004).
[7] A. Yoshimori, Phys. Rev. E **71,** 031203 (2005).
[8] G.K.-L. Chan and R. Finken, Phys. Rev. Lett. **94,** 183001 (2005).
[9] J. Dzubiella and C. N. Likos, J. Phys.: Condens. Matter **15,** L147 (2003).
[10] F. Penna and P. Tarazona, J. Chem. Phys. **119,** 1766 (2003).
[11] F. Penna, J. Dzubiella, and P. Tarazona, Phys. Rev. E **68,** 061407 (2003).
[12] J. Dzubiella, H. Löwen, and C. N. Likos, Phys. Rev. Lett. **91,** 248301 (2003).
[13] A. J. Archer and R. Evans, J. Chem. Phys. **121,** 4246 (2004).
[14] A. J. Archer, J. Phys.: Condens. Matter **17,** 1405 (2005).
[15] M. Rex, H. Löwen, and C. N. Likos, Phys. Rev. E **72,** 021404 (2005).
[16] C. N. Likos, Phys. Rep. **348,** 267 (2001).
[17] H. Löwen, Phys. Rep. **237,** 249 (1994).
[18] M. Medina-Noyola, Phys. Rev. Lett. **60,** 2705 (1988).
[19] G. Nägele, B. Steininger, U. Genz, and R. Klein, Phys. Scr. **55,** 119 (1994).
[20] W. B. Russel, D. A. Saville, and W. R. Schowalter, *Colloidal Dispersions* (Cambridge University Press, Cambridge, 1989).
[21] J. K. G. Dhont, *An Introduction to Dynamics of Colloids* (Elsevier, Amsterdam, 1996).
[22] A. A. Louis, P. G. Bolhuis, J.-P. Hansen, and E. J. Meijer, Phys. Rev. Lett. **85,** 2522 (2000).
[23] A. Jusufi, J. Dzubiella, C. N. Likos, C. von Ferber, and H. Löwen, J. Phys.: Condens. Matter **13,** 6177 (2001).
[24] C. N. Likos, M. Schmidt, H. Löwen, M. Ballauff, D. Pötschke, and P. Lindner, Macromolecules **34,** 2914 (2001).
[25] C. N. Likos, S. Rosenfeld, N. Dingenouts, M. Ballauff, N. Werner, and F. Vögte, J. Chem. Phys. **117,** 1869 (2002).
[26] I. O. Götze, H. M. Harreis, and C. N. Likos, J. Chem. Phys. **120,** 7761 (2004).
[27] M. Konieczny, C. N. Likos, and H. Löwen, J. Chem. Phys. **121,** 4913 (2004).
[28] A. Lang, C. N. Likos, M. Watzlawek, and H. Löwen, J. Phys.: Condens. Matter **12,** 5087 (2000).
[29] C. N. Likos, A. Lang, M. Watzlawek, and H. Löwen, Phys. Rev. E **63,** 031206 (2001).
[30] A. A. Louis, P. G. Bolhuis, and J.-P. Hansen, Phys. Rev. E **62,** 7961 (2000).
[31] A. J. Archer and R. Evans, Phys. Rev. E **64,** 041501 (2001).
[32] A. J. Archer and R. Evans, J. Phys.: Condens. Matter **14,** 1131 (2002).
[33] A. J. Archer, C. N. Likos, and R. Evans, J. Phys.: Condens. Matter **14,** 12031 (2002).
[34] A. J. Archer, R. Evans, and R. Roth, Europhys. Lett. **59,** 526 (2002).
[35] A. J. Archer, C. N. Likos, and R. Evans, J. Phys.: Condens. Matter **16,** L297 (2004).
[36] W. H. Press, S. A. Teukolosky, W. T. Vetterling, and B. P. Flannery, *Numerical Recipes in C* (Cambridge University Press, Cambridge, 1995).
[37] D. L. Ermak, J. Chem. Phys. **62,** 4189 (1975).
[38] M. P. Allen and T. J. Tildesley, *Computer Simulation of Liquids* (Clarendon, Oxford, 1989).